Aeolian mass flux characterization: uncertainties from a wind-tunnel perspective and implications for field studies

Aeolian sediment traps are widely used to estimate the total volume of wind-driven sediment transport, but also to study the vertical mass distribution of a saltating sand cloud. The reliability of sediment flux estimations from this data are dependent upon the specific configuration of the measurement compartments and the analysis approach used. In this study, we analyse the uncertainty of these measurements by investigating the vertical cumulative probability distribution and relative sediment flux derived from both wind-tunnel and field studies. Three existing datasets were used in combination with a newly acquired meteorological dataset, which was collected in combination with sediment fluxes from six different events, using three customized catchers at one of the beaches of Ameland in the north of The Netherlands. Fast-temporal data collected in a wind-tunnel shows that eq has a scattered pattern between impact and fluid threshold, but increases linearly with shear velocities above the fluid threshold. For finer sediment fractions, a larger portion of the sediment was transported closer to the surface compared to coarser sediment fractions. It was also shown that errors originating from the the distribution of the sampling compartments, specifically the location of the lowest sediment trap relative to the surface, can be identified using the relative sediment flux. In the field, surface conditions such as surface moisture, surface crusts or frozen surfaces have a more pronounced, but localized effect, than shear velocity. Uncertainty in aeolian mass flux estimates can be reduced by placing multiple compartments in closer proximity to the surface.

PeerJ PrePrints | http://dx.doi.org/10.7287/peerj.preprints.278v1 | CC-BY 4.0 Open Access | received: 7 Mar 2014, published: 7 Mar 2014

Aeolian mass flux characterization: uncertainties from a wind-tunnel perspective and implications for field studies

A. Poortinga*[1], J. Keijsers[2], J. Maroulis[3], and S.M. Visser[4]

[1]**Soil Physics and Land Management Group, Wageningen University, P.O. Box 47, 6700 AA Wageningen, The Netherlands**
[2]**Soil Physics and Land Management Group, Wageningen University, P.O. Box 47, 6700 AA Wageningen, The Netherlands**
[3]**Soil Physics and Land Management Group, Wageningen University, P.O. Box 47, 6700 AA Wageningen, The Netherlands**
[3]**Faculty of Science, Health, Education and Engineering, University of the Sunshine Coast, Locked Bag 4, Maroochydore DC, Queensland, 4588, Australia**
[4]**Team Soil Physics and Land Use, Alterra - Wageningen University and Research Center, P.O.Box 47, 6700 AA Wageningen, The Netherlands**

ABSTRACT

Aeolian sediment traps are widely used to estimate the total volume of wind-driven sediment transport, but also to study the vertical mass distribution of a saltating sand cloud. The reliability of sediment flux estimations from this data are dependent upon the specific configuration of the measurement compartments and the analysis approach used. In this study, we analyse the uncertainty of these measurements by investigating the vertical cumulative probability distribution and relative sediment flux derived from both wind-tunnel and field studies. Three existing datasets were used in combination with a newly acquired meteorological dataset, which was collected in combination with sediment fluxes from six different events, using three customized catchers at one of the beaches of Ameland in the north of The Netherlands. Fast-temporal data collected in a wind-tunnel shows that $\widetilde{q}$ has a scattered pattern between impact and fluid threshold, but increases linearly with shear velocities above the fluid threshold. For finer sediment fractions, a larger portion of the sediment was transported closer to the surface compared to coarser sediment fractions. It was also shown that errors originating from the the distribution of the sampling compartments, specifically the location of the lowest sediment trap relative to the surface, can be identified using the relative sediment flux. In the field, surface conditions such as surface moisture, surface crusts or frozen surfaces have a more pronounced, but localized effect, than shear velocity. Uncertainty in aeolian mass flux estimates can be reduced by placing multiple compartments in closer proximity to the surface.

Keywords: Sediment catchers, Measurements, Analysis method, Quality control, Non-linear regression analysis, trap elevation

INTRODUCTION

Aeolian sediment transport is an important geomorphological process that shapes a number of landscapes including coastal (e.g. Arens (1996); Wal (2000); Jackson and Nordstrom (2011),drift sand (Riksen et al., 2006; Riksen and Goossens, 2007) and deserts (e.g Bagnold (1941); Wiggs (2001)), and also agricultural areas (e.g. Visser and Sterk (2007a); Chepil and Woodruff (1963); Visser and Sterk (2007b)). Along sandy coasts, aeolian processes drive the morphological development of coastal dunes that protects the hinterland against flooding. Maintaining the natural aeolian dynamics allows vegetation to flourish in different successive stages, creating an appealing area for tourism and recreation (Poortinga et al., 2011). In agricultural areas, however, aeolian processes are often erosive, as fertile top soil is highly susceptible to wind erosion (Nanney et al., 1993). Therefore, an in-depth understanding of the physical processes of

wind-driven sediment transport is critically important.

Methods to study aeolian sediment transport include passive sediment traps (Rasmussen and Mikkelsen, 1998; Dong et al., 2004; Sterk and Raats, 1996; Basaran et al., 2011; Mendez et al., 2011), active samplers such as acoustic samplers (Spaan and van den Abeele, 1991; Yurk et al., 2013; Ellis et al., 2009b; Schönfeldt, 2012), laser particle counters (Hugenholtz and Barchyn, 2011; Sherman et al., 2011), piezoelectric samplers Baas (2004); Stout (1998), pressure sensitive samplers Ridge et al. (2011) and terrestrial laser scanners Nield and Wiggs (2011). The physics of wind blown sand are often studied in the controlled environment of a wind-tunnel (e.g. Youssef et al. (2008, 2012); Van Pelt et al. (2009); Goossens et al. (2000); Butterfield (1999) but also directly in the field (e.g. Namikas (2003); Ellis et al. (2012)). However, results from wind-tunnel studies can not be directly translated into field situations, as variability in environmental factors such as surface moisture, wind direction and velocity, bed elevation, vegetation, sediment composition, lag deposits, surface crusts and fetch play an important role. Despite recent progress in rapid data collection, passive sediment catchers are still frequently used to study aeolian sediment flux.

Passive sediment traps consist of various compartments located at different elevations. The sediment captured within these compartments, provides valuable information about the vertical sediment flux distribution (Ni et al., 2003; Dong et al., 2003; Butterfield, 1999), which is frequently used to estimate total sediment transport (Sterk et al., 1996, 2012; Sterk and Spaan, 1997; Visser et al., 2004a). However, passive sediment traps have some inherent uncertainties depending on the specific distribution of the compartments and their elevation above the surface, whereas sediment mass, inlet diameter, vertical position of the catchers, trapping efficiency, horizontal spacing between catcher arrays and wind direction were also identified as potential sources of uncertainty (Tidjani et al., 2011). Poortinga et al. (2013) collected data on the vertical distribution of sediment transport using a combination of active (saltiphones) and passive samplers. The aim of this study was to analyse uncertainties resulting from the distribution of the different trapping compartments and the influence of base elevation.

Fast-temporal data from the saltiphones were used to study uncertainties resulting from the distribution of the different sediment trapping compartments and the influence of base elevation. Implications for field studies were investigated using data from two published studies and one newly collected data-set, where three different customized sediment catchers were used. Moreover, the newly collected data was used to investigate the variability in vertical sediment flux and total sediment transport.

MATERIALS AND METHODS

Data collection

Data from three published studies and a new dataset were collected. Specific details about the locations and data collection methods used in the three published studies can be found in Poortinga et al. (2013), Farrell et al. (2012) and Visser et al. (2004b), while the data collection procedure used for the new dataset is presented below.

Study area

The research took place from November to December 2010 on a beach at the north-western end of Ameland, one of the West-Frisian barrier islands located in the northern extremity of The Netherlands (Fig 1(a)). The site is characterized by strong wind and wave dynamics in constructing bedforms and embryonic dune development. Human influence on this part of the beach is minimal compared to the middle section of the island. The study area is located East of a sand bar, which attached to the island in the mid 1980s, causing a progressive, attenuating sand wave to the East (Kwok et al., 2007).

Experimental setup

Data was obtained on sediment characteristics, sediment transport and a number of significant meteorological parameters. To determine sediment size, samples were taken from the surface of the beach at a number of locations and mixed into one large sample. This sample was dried and sieved in fractions of 50, 100, 250, 500, 1000 and 2000 μm. The median diameter was determined at 180 μm. Surface sands are largely composed of unconsolidated quartz grains with some feldspar and a small fraction of heavy minerals (Wal, 2000).

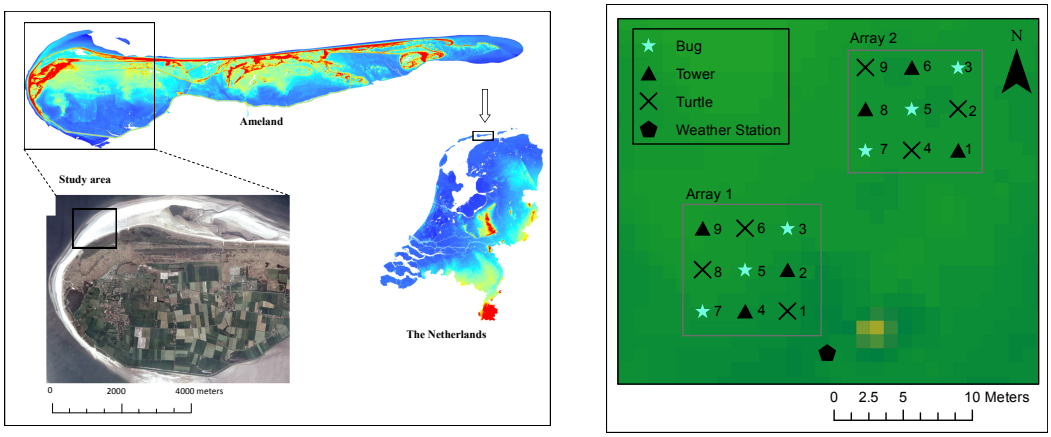

(a) The study area

(b) Field Experiment plots

Figure 1. Right image: Location of study area in the Netherlands (right), on the island of Ameland (top) and in the aerial photo of the western part of Ameland (left). Left image: the setup of the field experiment with the specific configuration of the equipment.

Measurement of sediment flux

Sediment flux was measured using the Modified Wilson and Cook sediment catchers (MWAC). These catchers are designed and used for capturing sediment with a sediment size ranging from dust to sand. The original design (Wilson and Cooke, 1980) contained six plastic bottles with glass inlets and outlets, placed horizontally at six heights between 0.15 and 1.52 m. These bottles were mounted on a rotating pole with a wind vane. Later studies (e.g. Sterk and Raats, 1996) used the same principle, but placed the bottles vertically instead of horizontally (Fig. 2(a)). Under beach conditions, aeolian sediment transport is solely governed by saltation, which seldom reaches heights above 15-20 cm. A traditional MWAC sediment catcher would therefore only capture sediment in the lower two or three bottles. This generates significant uncertainty in the analysis, as sediment flux is calculated based solely upon the fitting of an exponential curve through only two or three data points. Therefore, three different designs were introduced (Fig. 2), with all designs being based upon the traditional MWAC, but with all bottles mounted below 25 cm. The first design, nicknamed the ”Bug” (Fig. 2(b)), consists of two stacks of three bottles opposite each other, with their inlets at approximately the same height. The bottles are fixed to a wooden plate with an iron thread, so that the vertical distance between two inlets is approximately 5 cm. This design allows for the collection of more measurement points in case of any small horizontal variations in sediment flux, thereby reducing any uncertainty in flux calculations. The second design (Turtle) (Fig. 2(c)) consists of two bottles on each side, located at various heights. In this design, the bottles are fixed in the original clips, resulting in a larger vertical spacing of approximately 8 cm. For both designs, the horizontal distance between the inlets is approximately 22 cm. The Tower design (Fig. 2(d)) represents the more traditional setup with three or four bottles stacked above each other. The vertical spacing between the bottles is approximately 5 cm, as the bottles are once again, fixed to a wooden plate with iron thread instead of the conventional clip.

To evaluate the differences between the three new designs, they were placed in a 3 x 3 grid and separated by a distance of approximately 3 m. After the first event, an additional array of MWAC’s was installed approximately 8 m from the first array in order to obtain more measurements (Fig. 1(b)). To ensure a careful monitoring of the experiment, this second array was only installed when environmental conditions were favourable. Each array contained three catchers of each type. They were placed in a relatively flat and homogeneous part of the beach to ensure that the measured sediment flux was uniformly distributed. The elevation of the bottles relative to ground level, was measured to an accuracy of 1 mm after installation and before removal of the bottles.

Weather data

A meteorological station with four anemometers was arranged as a vertical array on a tower, which also included a wind vane, tipping bucket and two saltiphones (Spaan and van den Abeele, 1991) was

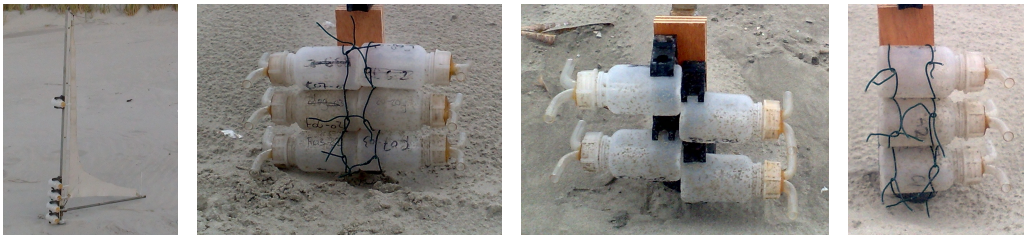

(a) Traditional design (b) Bug (c) Turtle (d) Tower

Figure 2. The traditional MWAC design with the three new designs.The traditional design (a) consists of 5 bottles distributed over approximately 1 m, the Bug design (b) consists of a total of six bottles (three on each side), the Turtle design (c) consists of 4 bottles (two on each side) in the original clips and the Tower design (d) consists of three bottles mounted above each other.

installed in the field directly on the beach in the middle of the study area (Fig. 1(b)), recording constantly throughout the period of investigation. The equipment was connected to a CR10 Campbell datalogger which recorded data every minute (Table 1). The on-site meteorological station contained 3 anemometers, measuring the wind speed at elevations of 0.54, 1.15 and 1.76 m. Pulses from the anemometer were averaged over the recording period and registered as average wind velocities per minute. Wind direction was measured using the wind vane at a height of approximately 2.5 m, while the tipping bucket recorded rainfall to an accuracy of 0.2 mm.

Table 1. Type, number and temporal resolution of instruments used during the field experiment on Ameland. The spatial distribution is shown in figure 1(b)

Instrument	number	use	temporal resolution
Anemometers	4	Wind velocity profile	1 minute
Windvane	1	wind direction	1 minute
Tipping bucket	1	amount of rainfall	1 minute
Saltiphones	2	transport intensity	1 minute
MWAC's	18	sediment flux	event

In order to capture the temporal variability in transport intensity, two saltiphones were placed close to the surface at different locations in the experimental area (Fig. 1(b)). The saltiphones were also connected to a CR10 datalogger with a digital pulse output signal, which for every second, the cumulative number of hits for that second were recorded.

Data analysis

The approach deployed by Dong et al. (2003); Dong et al. (2004) was utilised in this study, as their sediment trap contained a large number of compartments.

The vertical distribution of aeolian mass flux

When using passive sediment traps, sediment is trapped in different compartments that are located at different elevations above the surface. Sediment from each compartment was weighed and then plotted against elevation from which a non-linear regression is calculated to estimate total sediment transport. Despite various thoughts on whether to use an exponential, power of five parameter regression curve, the recent literature (Ellis et al., 2009a; Barchyn et al., 2011) suggests that an exponential decay function (equation 1) is most appropriate to describe aeolian sediment transport.

$$q_z = q_0 e^{-\beta z} \tag{1}$$

Equation 1 is used to determine the coefficients q_0 and β, also referred to as the portion of creep (q_0) and decay (β), where z (m) represents the elevation and q_z (kgm^{-2}) the amount of sediment at elevation z. Regression coefficients q_0 and β can subsequently be used to calculate the total amount of sediment transport Q (kgm^{-1}). This is done by the integral of equation 1 over the height of the saltation layer. The cumulative distribution function (CDF) of an aeolian mass flux (P_q) can be described by equation 2, using coefficient β found in equation 1. Figure 3 illustrates the relative sediment flux (black line) and the CDF (green line). When studying the characteristics of aeolian sediment flux, the CDF is preferred to the relative sediment flux, as this function is independent of the number of measurement points. Moreover, only coefficient β is used in the calculation, and therefore, the shape of the CDF is only determined by the specific mass distribution between the different compartments and not by the compartments elevation above the ground.

$$P_q = 1 - e^{-\beta z} \tag{2}$$

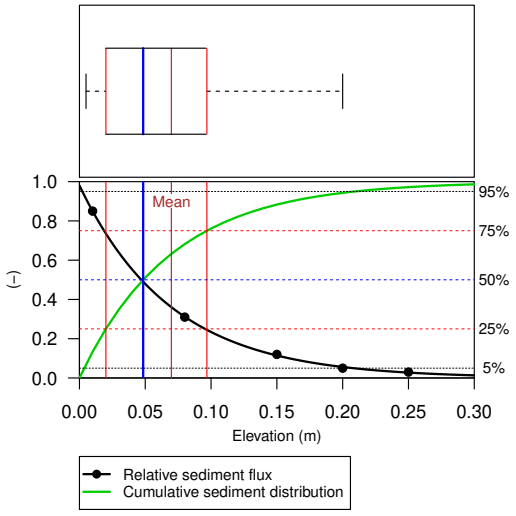

Figure 3. The vertical distribution of a relative aeolian sediment flux (points), the non-linear regression (equation 1) fitted through the data-points and the cumulative sediment distribution calculated from regression coefficient β. The median (blue, equation 4), mean (brown, equation 3), upper and lower quantile (red, equation 5 and 6) are also shown as a boxplot.

Besides the CDF, coefficient β (equation 1) can also be used to determine the mean (equation 3), median (equation 4), lower quartile (equation 5) and upper quartile (equation 6). Figure 3 shows the distribution function as a box-plot (top) and also for the relative sediment flux and CDF (bottom). The difference between the mean (brown line) and median (blue line), is that, given a probability $P(x)$, the mean is calculated by the integral $\int_{-\infty}^{\infty} xP(x)\,dx$ and the median by the point where the integral is 0.5 ($\int_{-\infty}^{\infty} xP(x)\,dx = 0.5$). The median splits the CDF into two equal parts, whereas the mean describes the point where the CDF would balance. As the median is less sensitive for outliers compared to the mean, we make use of the median.

$$\bar{q} = \frac{1}{\beta} \tag{3}$$

$$\widetilde{q} = \frac{ln(2)}{\beta} \tag{4}$$

$$q_{25} = \frac{ln(\frac{4}{3})}{\beta} \tag{5}$$

$$q_{75} = \frac{ln(4)}{\beta} \tag{6}$$

Dong et al. (2003) performed a series of wind-tunnel experiments to investigate the flux profile of wind-blown sand. They used a similar approach as describe in this study, however, they determined the cumulative mass distribution from the measured data. Moreover, they used the equation $q_z = q_0 e^{-b/z}$, where the regression coefficient β (here given as b) is divided by the elevation instead of multiplying (equation 1). Regression parameter β (as in equation 1) can be calculated by $\beta = 1/b$. The $\widetilde{q}$ for the different sediment size fractions and wind velocities, using β, is shown in Figure 4.

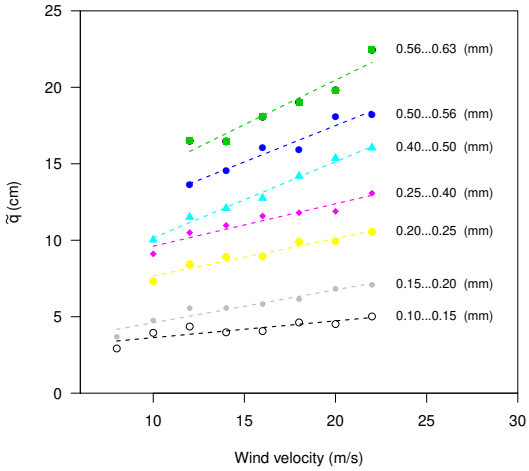

Figure 4. The $\widetilde{q}$ for different sediment fractions and wind velocities. The data was recalculated from Dong et al. (2003).

Figure 4 shows the variation in $\widetilde{q}$ for the various sediment size fractions over a range of wind speeds, especially where coarser sediments are transported at higher elevations. Furthermore, the $\widetilde{q}$ increase is more pronounced with higher wind velocities. For coarser sediments, the increase in $\widetilde{q}$ at high wind velocities is even greater.

Uncertainties in estimation of aeolian mass flux

Ellis et al. (2009a) identified three common methodological inconsistencies and thus sources of uncertainty in measuring aeolian sediment transport using passive traps. These include: (1) inconsistent representation of sediment trap elevations; (2) erroneous or sub-optimal regression analysis; and (3) inadequate or ambiguous bed elevation measurements.

In addition, the number of trapping compartments and location of the lowest sediment trap are also important considerations. Results of Dong and Qian (2007) were used to illustrate how the base elevation and number of traps affects the sediment flux estimation. They made use of a WITSEG sampler (Dong et al., 2004), which is a vertically integrated wedge shaped trap with 60 different compartments, where the lowest orifice can be aligned with the surface. The high data density of the WITSEG is advantageous when interested in a detailed description of the vertical mass distribution,

Dong and Qian (2007) determined the relative sediment flux, using equation 7, where the relative sediment flux (qr_z) at height (z) is calculated by dividing the measured sediment flux (qz) by the total amount of sediment (Q) collected within all compartments. After fitting a non-linear regression (equation 1) through the relative sediment flux data, they found a linear correlation between the regression coefficients q_0 (portion of creep) and β (decay function).

$$qr_z = \frac{qz}{Q}, Zr = \frac{z}{Z} \tag{7}$$

Figure 5 displays the dimensionless regression coefficients q_0 and β. Using the elevation data of the different compartments, we calculated the relative regression coefficient q_0 for a sequence of β's, while changing the elevation from the base (lines with different colors), but using the same distribution of compartments. Measurements using the WITSEG were taken between 0-1 cm, which is in agreement with the experiments. Here, it is important to note the difference in shape between the different base elevation lines. When measurements are taken close to the surface, the correlation between q_0 and β is almost linear, for the domain under consideration. However, when moving further away from the surface, the relationship becomes log-linear (Figure 5). This has large implications in terms of generating uncertainty in the estimation of q_0. Where measurements are taken further away from the surface, a small error in the calculation of β has even greater implications on estimating q_0 compared to where measurements are taken closer to the surface. An under- or overestimation in the q_0 regression parameter can have a significant effect on the determination of the total mass flux.

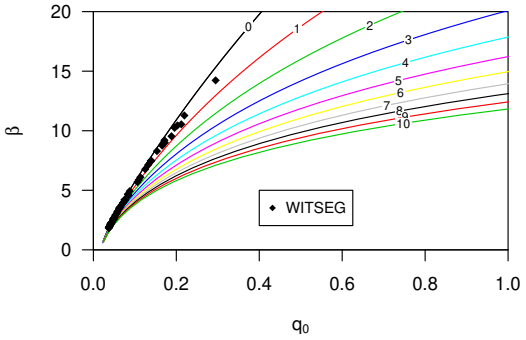

Figure 5. The regression coefficients q_0 and β calculated from the relative sediment flux (equation 7) for the WITSEG (data from Dong et al. (2004)). The coloured lines represent the relation between the q_0 and β for different base elevation (the number on the in line in cm), also calculated using the relative sediment flux.

The vertical cumulative mass distribution of the aeolian mass flux was investigated for each of the previous studies. Furthermore, we also evaluated the estimates of base elevation and any uncertainty of these measurements. For the newly collected dataset, the spatial variability was investigated for $\widetilde{q}$ and Q. Spatial variability was mapped using an inverse-distance weighting algorithm, with a minimum of three and a maximum of eight neighbours.

RESULTS AND DISCUSSION

Wind tunnel data

Data from Poortinga et al. (2013), collected in a wind-tunnel, was used to investigate the CDF of an aeolian saltation cloud. This dataset contains information on the different types of sediment catchers, sediment loss calculated from the saltiphones, and the total amount of sediment loss logged using a balance. The normalized sediment flux and CDF, calculated from four saltiphones (the highest located at 25 cm above the surface), are shown in Figure 6. The fit between the non-linear regression line and calculated sediment flux was $r^2 = 0.99$ on average, with a minimum $r^2 = 0.96$. The data was divided into high wind velocities (left in Fig. 6) and low wind velocities (right in Fig. 6), where the s50, s60 and s80 represent different sediments with a $d50$ of 285, 230 and 170 μ, respectively. The s80 (finer) sediment gets transported closer to the surface than coarser sediment fractions (s50 and s60), which is in agreement with the literature (Farrell et al., 2012; Dong et al., 2003; Dong and Qian, 2007). At higher wind velocities, more sediment is transported closer to the surface, except for the s80 (fine) sediment, as these particles are transported closer to the surface. Furthermore, $\widetilde{q}$ and shear velocities varied between the different experiments.

The use of saltiphones in fast-temporal aeolian sediment flux data, calculating sediment flux every

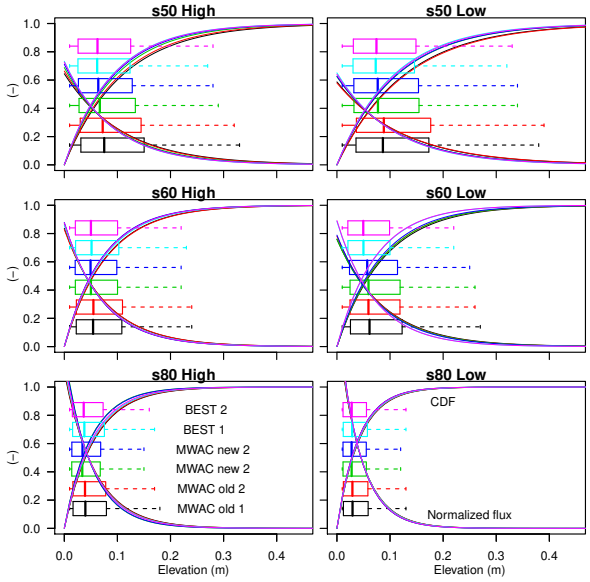

Figure 6. The relative sediment flux (equation 7) and CDF (equation 2) for three different types of sediment (s50,s60 and s80), three different sediment catchers (MWAC old, MWAC new and BEST) under high and low wind velocities.

second, was also deployed to investigate in detail the vertical sediment dynamics. Non-linear regression (equation 1) was applied to the data points and all the fluxes and for all data with $R^2 > 0.98$, the β was used to calculate $\widetilde{q}$ (equation 4). In Figure 7, $\widetilde{q}$ is plotted against shear velocity for experiments under high (left) and low wind velocities (right). As in Figure 6, finer sediment has a lower median $\widetilde{q}$. Despite considerable scatter, the median $\widetilde{q}$ values increase with increasing shear velocities. In the region between the impact (vertical black dotted line: Fig. 7) and fluid thresholds (green dotted line), the scatter is considerable. This scatter (indicated with an alpha color), represents measurements with low sediment flux which is more pronounced in low wind velocities. A linear regression curve was calculated for the high and low wind shear velocities (straight line), but also for the combination of high and low velocities (dotted line). All plots show a positive correlation between shear velocity and median $\widetilde{q}$, with coefficients 0.11, 0.051 and 0.18 for the s80, s60 and s50 sediment sizes, respectively.

In the wind tunnel experiment, three different type of sand catchers were used: the MWAC old, MWAC new and BEST (cf. Poortinga et al. (2013)). The findings in Figure 7 were used to validate the results of these sediment catchers. First, the $\widetilde{q}$ of the measured sediment flux was calculated for every experiment. Second, the $\widetilde{q}$ based on the mean shear velocity during the experiment, was calculated using the data from Figure 7. Figure 8 (top) shows $\widetilde{q}$ based on the values of the sediment catchers (before) and the values calculated from the saltiphones data (after). Differences between the two values increase from coarse to finer sediment. For the measurements using BEST, the differences are generally larger than the other catchers (Fig. 8).

To test whether $\widetilde{q}$ calculated from the saltiphones (Fig. 8: top) give a better approximation of the total sediment flux, it was used as a reference point to reposition the base elevation; with the difference between the sediment catcher guiding the repositioning of the traps. The sediment flux was recalculated using this new base elevation. New sediment fluxes were then compared with sediment loss as registered by a balance. Figure 8 (bottom) shows the efficiency of the initial sediment flux estimation (red) and the newly calculated sediment flux (green), where 100% is an exact match with the balance. Some 29 of the 36 measurements were shown to indicate an improvement (Fig. 8). In general, improvements are considerable, and a decrease in efficiency is minimal. For finer sediment, improvements were even higher when compared to coarser sediment.

The relative sediment flux of the saltiphones and sediment catchers were used to determine q_0 and β

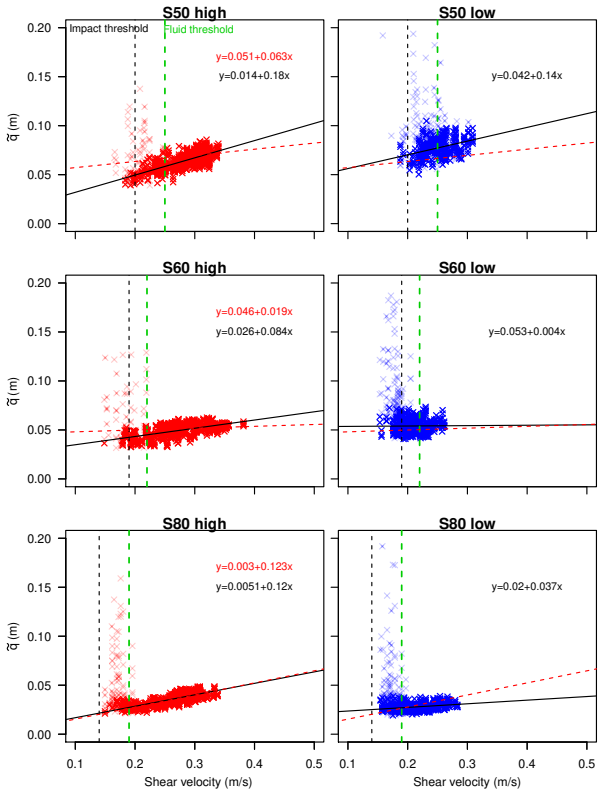

Figure 7. The shear velocity versus the $\widetilde{q}$ for three different types of sediment (s50,s60 and s80) under high and low wind velocities.

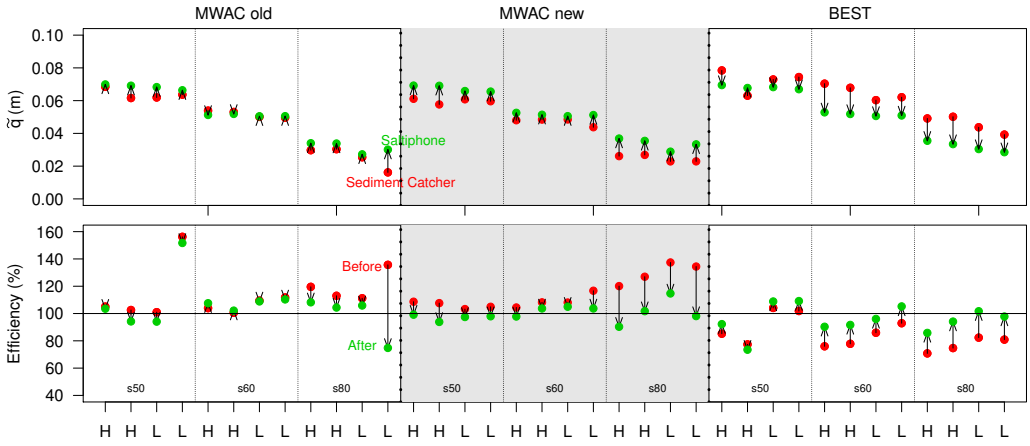

Figure 8. The $\widetilde{q}$ from the saltiphones compared with the $\widetilde{q}$ of the sediment catcher (top) and the recalculated efficiency (bottom) using the $\widetilde{q}$ as a reference. Data is shown for three different sediment catchers (MWAC old, MWAC new and BEST), three different types of sediment (s50,s60 and s80) under high (H) and low (L) wind velocities. During the experiment, the sediment catcher and saltiphones were located next to each other. The arrows (top) indicate the shift in $\widetilde{q}$ used to calculate the new base elevation. The arrows (bottom) indicate the change in efficiency.

(Fig. 9). When the lowest saltiphones were located at 3 cm, we found a strong linear relationship between q_0 and β. Finer sediment had a larger range of regression coefficients, with higher values for β given that a higher proportion of sediment is transported closer to the surface. The intercept of the linear regression increases with coarser sediment, whereas the slope of the regression decreases. The difference between the intercept and slope of the s50 and s60 sediment is small. For passive sediment catchers, there is good agreement between the calculated base elevation and the experimental results (Fig. 9). The BEST catcher was located around 1.5 cm from the surface, whereas the lowest trap of the MWAC catchers was located between 4 and 5 cm. The mean measurement error was 1.3 mm with a maximum of 2.4 mm.

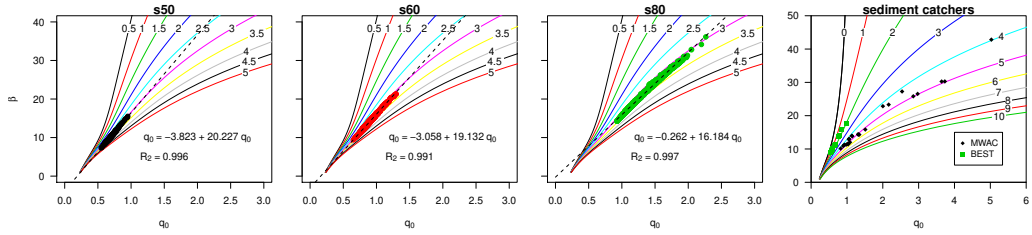

Figure 9. The q_0 and β, calculated from the relative sediment flux (equation 7) for different types of sediment (s50, s60, s80) using saltiphones data and for all measurements using passive sediment traps (the right image). The lines represent different base elevation.

The disagreement in vertical flux distribution between the saltiphones and sediment catchers, but also between sediment loss measured by the balance and the calculated flux from the sediment catchers, is mainly caused by the specific configuration of a sediment catcher. In fact, when applying an exponential regression function, the elevation, orientation and measurement accuracy of the lowest bottle determines the result to a large extent. Here, finer sediment is more susceptible to errors compared to coarser sediment. Figure 10, presents the experimental outputs when using the MWAC and BEST catchers with s80 (fine) sediment, highlighting the measured relative sediment fluxes (black dots), including the exponential regression (equation 1) and a linear regression. It can be seen that the BEST catcher contains one data-point below the $\widetilde{q}$ while the MWAC has none. The influence of the lowest data-point is significant, as it determines the intersection with the y-axis and thus the total sediment flux. As for fine sediment, errors will be more pronounced as a larger portion of the mass is transported close to the surface, there are small inconsistencies in the orientation of the catcher, and measurement issues occur with the elevation or difference in efficiency under different mass flux density. Applying a linear function to the points close to the surface, and a power function for the higher located points (cf. Poortinga et al. (2013)), will therefore give more coherent results, as the effect of the lowest point on the total mass flux is reduced. Moreover, Ni et al. (2003) showed that saltating grains follow an exponential decay function, whereas creeping and reptating grains deviate from it. The mathematical description might therefore also be a source of uncertainty.

Field data

Field studies do not have the advantage of a controlled environment where specific parameters can be fixed. Surface moisture and bedform development, for instance, are known as important limiting factors in sediment transport, and can negatively affect the measurements. Data from Farrell et al. (2012) were used in a re-analysis because their short-lived experiments contained several data-points close to the surface. For the sub-environment Cow Splat Flat Fine (CSFF), $\widetilde{q}$ were arranged according to date (Fig. 11 left) and q_0 and β were calculated for the relative flux (Fig. 11 right). For this sub-environment, the calculated elevation from the surface were in strong agreement with the measured values. The variation in $\widetilde{q}$ was best explained when arranging them according to measurement date, where no relation was found with shear velocity (ranging from 0.45 - 0.54 ms^{-1}) or grain-size. A logical explanation would be the impacts of the surface surface characteristics of such variables such as surface moisture and incipient bedform development. However, this is far from conclusive, as it was also found that $\widetilde{q}$ increased with a decreasing R^2 (ranging from 0.968 - 0.999). The same study also took three measurements at the beach sub-environment over two consecutive days. These measurement received specific attention, as they were

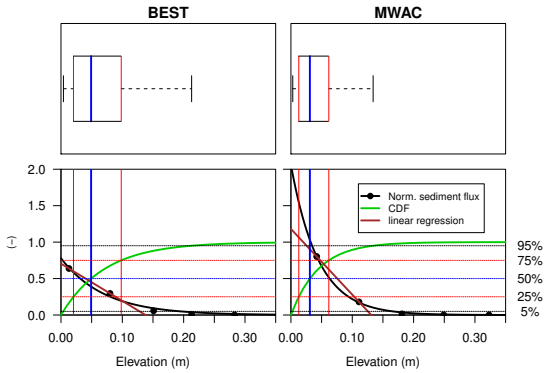

Figure 10. The vertical distribution of the relative aeolian sediment flux for the BEST and MWAC catcher. The dots indicate measurements (s80 sediment), the non-linear regression curve is shown in black and the CDF in green. Furthermore, a linear function was plotted through the two points located closest to the surface (brown). The $\widetilde{q}$ (blue, equation 4), $\bar{q}$ (brown, equation 3), upper and lower quantile (red, equation 5 and 6) are also shown as a boxplot.

taken at a wet and immobile foreshore without visible bedform deformation. We found $\widetilde{q}$ values of 3,7, 4.5 and 3.1 cm with R^2 of 0.966, 0.890 and 0.997, respectively. As this dataset only contains three data-points with varying R^2, it is difficult to draw conclusions based on $\widetilde{q}$ or measured base elevation.

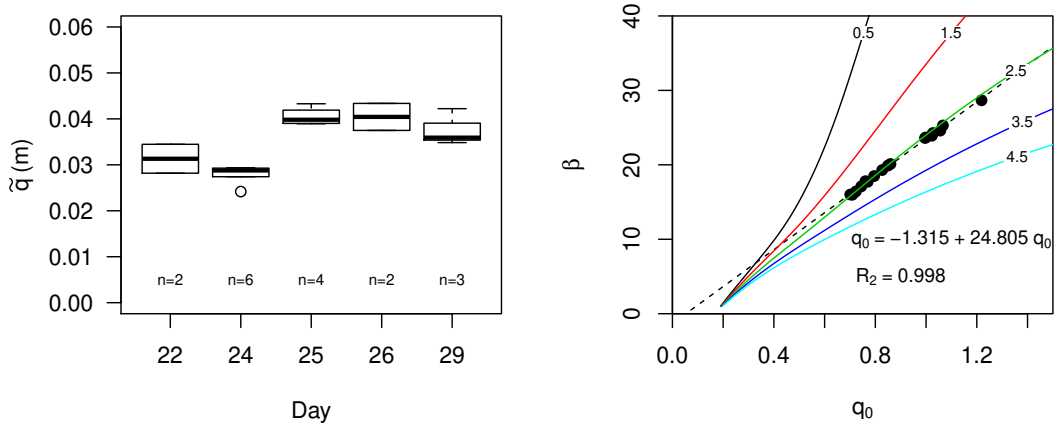

Figure 11. The $\widetilde{q}$ for experiments performed (at the sub-environment Cow Splat Flat Fine) on different days (left) and the q_0 and β for all events combined. Coloured lines represent different base elevation. Data was obtained from Farrell et al. (2012)

.

Visser et al. (2004b) conducted experiments on three different geomorphic units: degraded, valley and dune. Besides sand, the soils in this area also contained considerable quantities of silt: 19.4, 15.9 and 13.0% and clay 21.6, 5.1 and 3% for the degraded, valley and dune site, respectively. The study obtained results for 11 different events in the year 2001, with 17 MWAC catchers installed at each site. In order to remove uncertainty from the data while maintaining an acceptable number of data-points, measurements with $R^2 < 0.95$ were removed from the dataset. This is different from previous studies, where $R^2 < 0.98$ was used because measurements were taken over longer periods and when comparing the different units (Fig. 12: left), it was found that $\widetilde{q}$ is highest for the degraded site, followed by the valley and dune site.

The degraded and valley site have higher fractions of silt and clay, which are transported over higher elevations. However, surface crusts might also cause saltating particles to reach higher elevations. The variation in $\widetilde{q}$ within an event is generally low for the degraded and valley site, but slightly higher for the degraded site. The variation between events is also small, except for the events on 10 and 13 July. Here the values for $\widetilde{q}$ are high and have a large variation. During these events, large amounts of dust were transported through the study area. No clear relation was found between $\widetilde{q}$ and wind velocity.

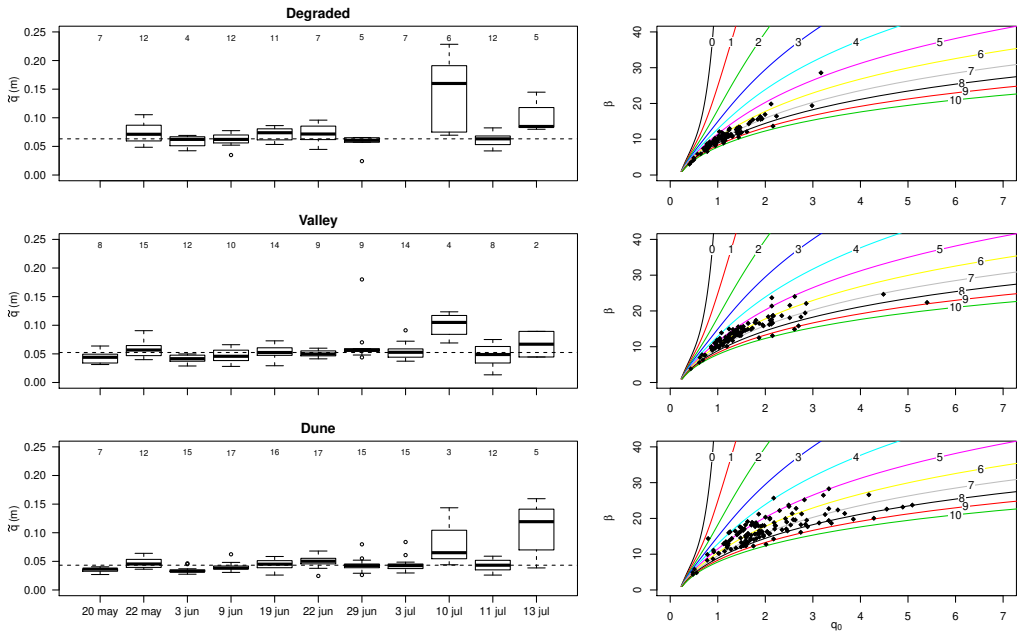

Figure 12. The $\widetilde{q}$ for 12 events in three different geomorphic units (left) and the relation between q_0 and β, where the lines represent different base elevations. Data was obtained from Visser et al. (2004b).

Figure 12 (right) shows q_0 and β, calculated from the relative sediment flux. As surface elevation varied for the different measurements, the points are plotted on different curves. Due to the lower decay rate (coefficient β) at the degraded site, points are still closely related. However, at the dune site sediment is transported closer to the surface, resulting in higher decay rates. As the lines spread with higher decay rates, there is higher spread in points. Compared to the degraded site, there is larger uncertainty in q_0 for the dune site, as small errors in β will result in larger errors in q_0 (Fig. 12).

Figure 13 displays the uncertainty in q_0 for one event (May 22) at the dune site. Here, the measured elevation is shown in red; where the elevation is based on the relative q_o and β, it is shown in green. For this event, all calculated elevations are lower compared to the measured. This indicates that there is a likely error in the measured base-elevation, leading to an overestimation of q_0. As expected, errors in q_0 are largest for the dune site, followed by the valley and degraded site. However, the larger error in q_0 does not directly correspond to a larger error in base elevation. Elevation here was estimated using $z = ln(q_z/q_0)/\beta$ (equation 1), with the higher decay rates at the dune site having a more pronounced effect on equation 1 than the larger range of q_0. For flux estimation, on the other hand, small changes in elevation have a much larger impact, as a greater portion of transport takes place close to the surface.

New data were collected for six different events (Table 2). The duration of the experiments varied from a few hours to two days. Phases of saltation were separated using the saltiphones data, where every minute more than 100 counts were logged. The shear velocity during these saltation periods varied between 0.30 - 0.41 ms^{-1}. Wind directions predominantly came from the E-NE while only event three had variable wind conditions (Table 2). Three events were characterized by rainfall, with a maximum of 9.8 mm during event three. Saltiphones data were also included as an indication of the degree of saltation activity.

Of the three catchers (turtle, spider and tower) used in the experiments, two of them contained

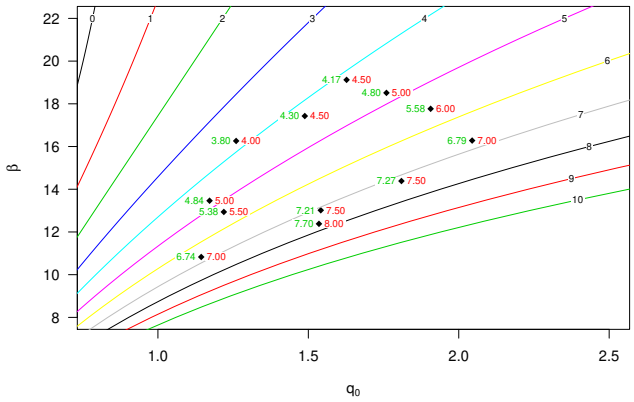

Figure 13. The q_0 and β calculated from the relative sediment flux for the Dune (May 22) site. The lines represent different base elevation, the red numbers are the measured elevation whereas the green values are the calculated elevations based on relative q_0 and β

Table 2. The meteorological conditions and saltation activity measured during the different at Ameland.

Event	duration (hour)	saltation (hour)	$\bar{U}_\star$ ms^{-1}	wind direction	Rainfall mm	saltiphone $counts\ sec^{-1}$	arrays
1	23.9	1.6	0.30	E	0.0	204	1
2	43.7	25.1	0.37	NE	0.4	924	2
3	42.4	5.7	0.41	variable	9.8	931	2
4	76.6	5.6	0.32	ENE	0.2	1140	1
5	5.4	4.5	0.33	ENE	0.0	714	2
6	3.3	3.2	0.40	ENE	0.0	984	2

compartments on both sides of the catchers. The impact of this horizontal variation on sediment flux was investigated by evaluating R^2 as a non-linear regression (equation 1) was applied to all measurements with at least four data-points. For the spider sampler, a non-linear regression was applied to both sides of the catcher, where the middle bottle of the opposite side was included. The results (Fig. 14(a)) show that the Tower has the best correlation, followed by the Turtle. The spider has the poorest performance but contains more measurements. Disturbance of the airflow might have caused the decrease in performance. In general, most measurements have a very high correlation, indicating only minor impacts of horizontal variability. However, to exclude the effect of horizontal variability and other sources of uncertainty, only measurement with an $R^2 > 0.98$ were included for further analysis.

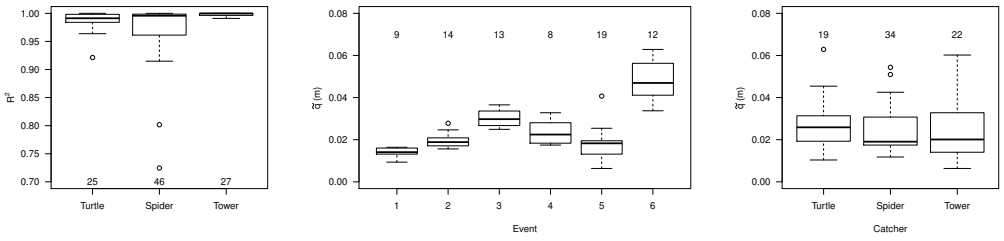

(a) R^2 (b) $\widetilde{q}$ according to event (c) $\widetilde{q}$ according to catcher

Figure 14. The R^2 for the different catchers (left), the $\widetilde{q}$ for every event (middle) and the $\widetilde{q}$ according to catcher (right).

The $\widetilde{q}$ values are shown in Figure 14(b). Values for event 6 are higher compared to other events, which is most likely caused by the frozen surface. During events experiencing rainfall, sediment was generally transported over higher elevations. However, the configuration of the traps on the catcher were also found to have an impact. Figure 14(c) shows that the the Turtle design gives generally higher values for $\widetilde{q}$ compared to the other two designs. This is caused by the point density being close to the surface. For the Spider and Tower designs, regression coefficient β is based on one point close to the surface, whereas the Turtle has two data points. The range in $\widetilde{q}$ is larger for the Tower compared to the Spider, as the Spider has two data points at approximately the same elevation, where the measurement is refuted when these points do not match. Measured base elevation was in good agreement with the calculated base elevation, with an average difference of 0.7 mm and a maximum of 5 mm; with the Turtle displaying the largest variation, followed by the Spider and the Tower.

An Inverse Distance Weighting (IDW) algorithm was used to investigate the spatial variability of $\widetilde{q}$ and Q (Fig. 15). We selected events 2, 3, 5 and 6, as during these experiments, two arrays of catchers were used. For all events, the lower-located array has lower values for $\widetilde{q}$ compared to the higher array. Based on observations, we can confirm that the surface of the upper array was generally wetter than the lower array. This is in line with other findings (Nield and Wiggs, 2011; Farrell et al., 2012), who also found that sediment is transported over higher elevations on wet surfaces. The spatial variability in saltation height (and thus surface characteristics) shows no alignment with the total transported sediment. Furthermore, the large variability in sediment flux between the different events, means there is also large variability in total sediment transport in individual events. Within the measurement plot, the peak values are eight times higher than the lowest values. In general, there is good agreement in measured sediment flux between points located close to each other. However, within meters of these measurements we can see major differences in total sediment flux. Besides the limiting effect of surface moisture on aeolian sediment transport (Namikas and Sherman, 1996; Cornelis and Gabriels, 2003; Neuman, 2003), the variability in sediment flux can be attributed to the presence of aeolian streamers (Baas and Sherman, 2005; Baas, 2008) and/or fetch length (Davidson-Arnott et al., 2005; Bauer et al., 2009; Delgado-Fernandez, 2010).

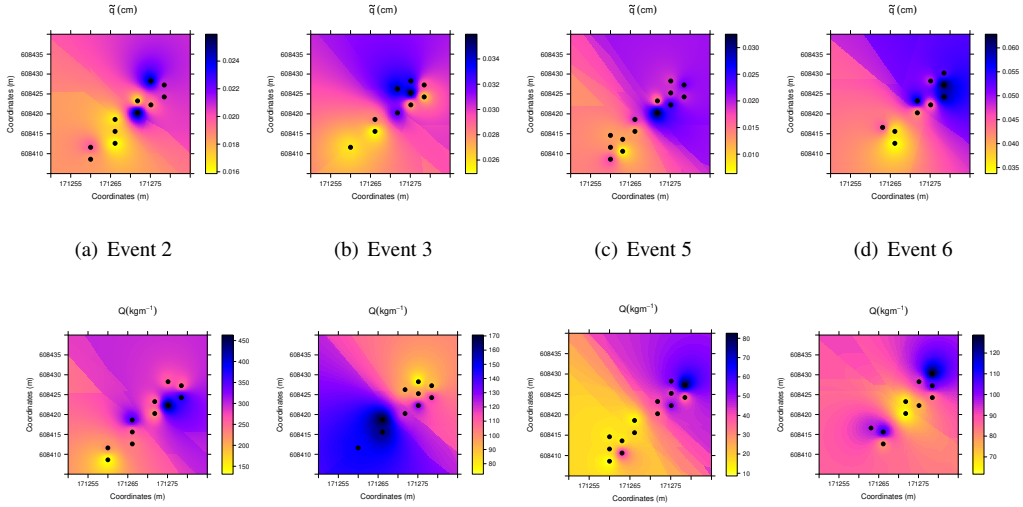

(a) Event 2 (b) Event 3 (c) Event 5 (d) Event 6

(e) Event 2 (f) Event 3 (g) Event 5 (h) Event 6

Figure 15. The spatial distribution of $\widetilde{q}$ (top) and Q (bottom) for events 2,3,5 and 6.

Differences in the vertical sediment flux as found in the wind-tunnel studies have limited validity for field studies, as surface conditions were found to have an important impact on saltation. Wet, frozen or crusted surfaces increase saltation height, as particles retain a higher proportion of their impact energy (Farrell et al., 2012). This effect was regarded as localized due to the spatial variability of the surface. Moreover, saltation trajectories were found to have a scattered pattern between impact and fluid threshold. This may impact results from the field, as during some events, transport was highly intermittent due to fluctuations in wind speed (Davidson-Arnott and Bauer, 2009; Stout and Zobeck, 1997). However,

fast-temporal field data is necessary to study this phenomena in more detail.

CONCLUSION AND RECOMMENDATIONS

Using fast-temporal data approaches on measuring aeolian sediment transport in a wind-tunnel, we found that $\widetilde{q}$ displays a scattered pattern between the impact and fluid threshold, but shows a linear increase with shear velocities above the fluid threshold. Furthermore, it was shown that errors that originate from the distribution of compartments and the location of the lowest sediment trap can be identified using the relative sediment flux. In field situations, shear velocity was not found to be the most import ant controlling factor in vertical sediment flux characterization. Instead, surface moisture was an important impact, although particle characteristics of the source area should also be considered. Errors have a more pronounced effect on sediment flux estimation for fine compared to coarse sediment, as for fine sediment fractions, a larger portion is transported closer to the surface. In order to reduce uncertainty, it is recommended to locate multiple traps closer to the surface.

ACKNOWLEDGMENTS

We would like to acknowledge to the following persons who have made the completion of the manuscript possible. Pierre Jongerius and Corjan Nolet, thanks for the hard labor in data collection.

REFERENCES

Arens, S. M. (1996). Rates of aeolian transport on a beach in a temperate humid climate. *Geomorphology*, 17(1-3):3 – 18. Response of Aeolian Processes to Global Change.

Baas, A. C. (2004). Evaluation of saltation flux impact responders (safires) for measuring instantaneous aeolian sand transport intensity. *Geomorphology*, 59(1–4):99 – 118.

Baas, A. C. (2008). Challenges in aeolian geomorphology: investigating aeolian streamers. *Geomorphology*, 93(1):3–16.

Baas, A. C. W. and Sherman, D. (2005). Formation and behavior of aeolian streamers. *Journal of Geophysical Research*, 110(F3):F03011.

Bagnold, R. A. (1941). *The physics of blown sand and desert dunes.* Methuen, London.

Barchyn, T. E., Hugenholtz, C. H., and Ellis, J. T. (2011). A call for standardization of aeolian process measurements: moving beyond relative case studies. *Earth Surface Processes and Landforms*, 36(5):702–705.

Basaran, M., Erpul, G., Uzun, O., and Gabriels, D. (2011). Comparative efficiency testing for a newly designed cyclone type sediment trap for wind erosion measurements. *Geomorphology*, 130(3-4):343–351.

Bauer, B., Davidson-Arnott, R., Hesp, P., Namikas, S., Ollerhead, J., and Walker, I. (2009). Aeolian sediment transport on a beach: surface moisture, wind fetch, and mean transport. *Geomorphology*, 105(1):106–116.

Butterfield, G. R. (1999). Near-bed mass flux profiles in aeolian sand transport: high-resolution measurements in a wind tunnel. *Earth Surface Processes and Landforms*, 24(5):393–412.

Chepil, W. and Woodruff, N. (1963). The physics of wind erosion and its control. *Advances in agronomy*, 15:211–302.

Cornelis, W. and Gabriels, D. (2003). The effect of surface moisture on the entrainment of dune sand by wind: an evaluation of selected models. *Sedimentology*, 50(4):771–790.

Davidson-Arnott, R. and Bauer, B. (2009). Aeolian sediment transport on a beach: Thresholds, intermittency, and high frequency variability. *Geomorphology*, 105(1–2):117 – 126.

Davidson-Arnott, R. G., MacQuarrie, K., and Aagaard, T. (2005). The effect of wind gusts, moisture content and fetch length on sand transport on a beach. *Geomorphology*, 68(1):115–129.

Delgado-Fernandez, I. (2010). A review of the application of the fetch effect to modelling sand supply to coastal foredunes. *Aeolian Research*, 2(2):61–70.

Dong, Z., Liu, X., Wang, H., Zhao, A., and Wang, X. (2003). The flux profile of a blowing sand cloud: a wind tunnel investigation. *Geomorphology*, 49(3):219–230.

Dong, Z. and Qian, G. (2007). Characterizing the height profile of the flux of wind-eroded sediment. *Environmental Geology*, 51:835–845.

Dong, Z., Sun, H., and Zhao, A. (2004). Witseg sampler: a segmented sand sampler for wind tunnel test. *Geomorphology*, 59(1–4):119 – 129.

Ellis, J., Li, B., Farrell, E., and Sherman, D. (2009a). Protocols for characterizing aeolian mass-flux profiles. *Aeolian Research*, 1(1–2):19 – 26.

Ellis, J. T., Morrison, R. F., and Priest, B. H. (2009b). Detecting impacts of sand grains with a microphone system in field conditions. *Geomorphology*, 105(1):87–94.

Ellis, J. T., Sherman, D. J., Farrell, E. J., and Li, B. (2012). Temporal and spatial variability of aeolian sand transport: Implications for field measurements. *Aeolian Research*, 3(4):379 – 387.

Farrell, E., Sherman, D., Ellis, J., and Li, B. (2012). Vertical distribution of grain size for wind blown sand. *Aeolian Research*, 7:51–61.

Goossens, D., Offer, Z., and London, G. (2000). Wind tunnel and field calibration of five aeolian sand traps. *Geomorphology*, 35(3):233–252.

Hugenholtz, C. H. and Barchyn, T. E. (2011). Laboratory and field performance of a laser particle counter for measuring aeolian sand transport. *Journal of Geophysical Research: Earth Surface (2003–2012)*, 116(F1).

Jackson, N. L. and Nordstrom, K. F. (2011). Aeolian sediment transport and landforms in managed coastal systems: A review. *Aeolian Research*, 3(2):181 – 196.

Kwok, F., Gerritsen, F., and Cleveringa, J. (2007). Morphodynamics and sand bypassing at ameland inlet, the netherlands. *Journal of Coastal Research*, 23(1):106–118.

Mendez, M., Funk, R., and Buschiazzo, D. (2011). Field wind erosion measurements with big spring number eight (bsne) and modified wilson and cook (mwac) samplers. *Geomorphology*, 129(1-2):43–48.

Namikas, S. L. (2003). Field measurement and numerical modelling of aeolian mass flux distributions on a sandy beach. *Sedimentology*, 50(2):303–326.

Namikas, S. L. and Sherman, D. J. (1996). A review of the effects of surface moisture content on aeolian sand transport. In *Desert Aeolian Processes*, pages 269–293. Springer.

Nanney, R., Fryrear, D., and Zobeck, T. (1993). Wind erosion prediction and control. *Water Science & Technology*, 28(3-5):519–527.

Neuman, C. M. (2003). Effects of temperature and humidity upon the entrainment of sedimentary particles by wind. *Boundary-Layer Meteorology*, 108(1):61–89.

Ni, J. R., Li, Z. S., and Mendoza, C. (2003). Vertical profiles of aeolian sand mass flux. *Geomorphology*, 49(3):205–218.

Nield, J. M. and Wiggs, G. F. (2011). The application of terrestrial laser scanning to aeolian saltation cloud measurement and its response to changing surface moisture. *Earth Surface Processes and Landforms*, 36(2):273–278.

Poortinga, A., van Minnen, J., Keijsers, J., Riksen, M., Goossens, D., and Seeger, M. (2013). Measuring fast-temporal sediment fluxes with an analogue acoustic sensor: A wind tunnel study. *PLoS ONE*, 8(9):e74007.

Poortinga, A., Visser, S. M., Riksen, M. J., and Stroosnijder, L. (2011). Beneficial effects of wind erosion: Concepts, measurements and modeling. *Aeolian Research*, 3(2):81–86.

Rasmussen, K. R. and Mikkelsen, H. E. (1998). On the efficiency of vertical array aeolian field traps. *Sedimentology*, 45(4):789–800.

Ridge, J. T., Rodriguez, A. B., Fegley, S. R., Browne, R., and Hood, D. (2011). A new 'pressure sensitive'method of measuring aeolian sediment transport using a gauged sediment trap (gast). *Geomorphology*, 134(3):426–430.

Riksen, M., Ketner-Oostra, R., Turnhout, C., Nijssen, M., Goossens, D., Jungerius, P., and Spaan, W. (2006). Will we lose the last active inland drift sands of western europe? the origin and development of the inland drift-sand ecotype in the netherlands. *Landscape Ecology*, 21(3):431–447.

Riksen, M. J. and Goossens, D. (2007). The role of wind and splash erosion in inland drift-sand areas in the netherlands. *Geomorphology*, 88(1–2):179 – 192.

Schönfeldt, H.-J. (2012). High resolution sensors in space and time for determination saltation and creep intensity. *Earth Surface Processes and Landforms*, 37(10):1065–1073.

Sherman, D. J., Li, B., Farrell, E. J., Ellis, J. T., Cox, W. D., Maia, L. P., and Sousa, P. H. (2011). Measuring aeolian saltation: a comparison of sensors. *Journal of Coastal Research*, pages 280–290.

Spaan, W. and van den Abeele, G. (1991). Wind borne particle measurements with acoustic sensors. *Soil Technology*, 4(1):51 – 63.

Sterk, G., Herrmann, L., and Bationo, A. (1996). Wind-blown nutrient transport and soil productivity changes in southwest niger. *Land Degradation and Development*, 7(4):325–335.

Sterk, G., Parigiani, J., Cittadini, E., Peters, P., Scholberg, J., and Peri, P. (2012). Aeolian sediment mass fluxes on a sandy soil in central patagonia. *Catena*, 95:112–123.

Sterk, G. and Raats, P. (1996). Comparison of models describing the vertical distribution of wind-eroded sediment. *Soil Science Society of America Journal*, 60(6):1914–1919.

Sterk, G. and Spaan, W. (1997). Wind erosion control with crop residues in the sahel. *Soil Science Society of America Journal*, 61(3):911–917.

Stout, J. and Zobeck, T. (1997). Intermittent saltation. *Sedimentology*, 44(5):959–970.

Stout, J. E. (1998). Effect of averaging time on the apparent threshold for aeolian transport. *Journal of Arid Environments*, 39(3):395 – 401.

Tidjani, A. D., Bielders, C., Rosillon, D., and Ambouta, K.-M. (2011). Uncertainties in plot-scale mass balance measurements using aeolian sediment traps. *Soil Science Society of America Journal*, 75(2):708–718.

Van Pelt, R., Peters, P., and Visser, S. (2009). Laboratory wind tunnel testing of three commonly used saltation impact sensors. *Aeolian Research*, 1(1-2):55–62.

Visser, S. and Sterk, G. (2007a). Nutrient dynamics - wind and water erosion at the village scale in the sahel. *Land Degradation and Development*, 18(5):578–588.

Visser, S. and Sterk, G. (2007b). Nutrient dynamics—wind and water erosion at the village scale in the sahel. *Land Degradation & Development*, 18(5):578–588.

Visser, S., Sterk, G., and Ribolzi, O. (2004a). Techniques for simultaneous quantification of wind and water erosion in semi-arid regions. *Journal of Arid Environments*, 59(4):699–717.

Visser, S. M., Sterk, G., and Snepvangers, J. J. (2004b). Spatial variation in wind-blown sediment transport in geomorphic units in northern burkina faso using geostatistical mapping. *Geoderma*, 120(1):95–107.

Wal, D. v. d. (2000). Grain-size-selective aeolian sand transport on a nourished beach. *Journal of Coastal Research*, 16(3):pp. 896–908.

Wiggs, G. (2001). Desert dune processes and dynamics. *Progress in Physical Geography*, 25(1):53–79.

Wilson, S. and Cooke, R. (1980). *Wind erosion.*

Youssef, F., Erpul, G., Bogman, P., Cornelis, W., and Gabriels, D. (2008). Determination of efficiency of vaseline slide and wilson and cooke sediment traps by wind tunnel experiments. *Environmental Geology*, 55(4):741–750.

Youssef, F., Visser, S. M., Karssenberg, D., Erpul, G., Cornelis, W. M., Gabriels, D., and Poortinga, A. (2012). The effect of vegetation patterns on wind-blown mass transport at the regional scale: A wind tunnel experiment. *Geomorphology*, 159:178–188.

Yurk, B. P., Hansen, E. C., and Hazle, D. (2013). A deadtime model for the calibration of impact sensors with an application to a modified miniphone sensor. *Aeolian Research*, 11:43–54.